Effect of mass extractions and injections on the performance of a fixed-size humidification-dehumidification desalination system

Gregory P. Thiel*, Jacob A. Miller*, Syed M. Zubair**, and John H. Lienhard V*

*Rohsenow Kendall Heat Transfer Laboratory, Department of Mechanical Engineering, Massachusetts Institute of Technology, Cambridge, MA 02139-4307, USA
**Department of Mechanical Engineering, King Fahd University of Petroleum and Minerals, Dhahran, Saudi Arabia

Abstract

The impact of mass extractions and injections as a method for increasing the energetic performance of fixed-size humidification-dehumidification desalination systems is examined. Whereas previous studies of this problem have been restricted to thermodynamic models, the use of a more complete model that includes transport provides the ability to quantify the impact of mass extractions/injections on a realizable, fixed-size system. For a closed air, open water cycle, the results show that a single water extraction from the dehumidifier to the humidifier increases the gained output ratio by up to 10%, with extractions higher in the cycle proving more effective. The sizing problem for the humidifier and dehumidifier under thermodynamically optimized conditions found in literature is also discussed, as is the impact of system size on overall performance of a system without extractions/injections. For a range of sizes, it is shown that a rough doubling of both dehumidifier and humidifier size results in a two- to three-fold increase in gained output ratio, with diminishing returns as the absolute sizes increase.

Keywords: Humidification-dehumidification; desalination; balancing; energy efficiency

Nomenclature

Roman Symbols

a	Packing specific area, m^2/m^3
A_c	Cross-sectional area, m^2
A_s	Surface area, m^2
C^*	Capacity rate ratio, $(\dot{m}c_p)_{\min}/(\dot{m}c_p)_{\max}$
c_p	Specific heat capacity, J/kg K
D	Hydraulic diameter, m
$\mathscr{D}$	Diffusion coefficient, m^2/s
GOR	Gained output ratio
h	Specific enthalpy, kJ/kg
h_{conv}	Convective heat transfer coefficient, W/m^2 K
h_{mass}	Convective mass transfer coefficient, kg/m^2 s
h_{fg}	Specific enthalpy of vaporization, kJ/kg
K	Humidifier mass transfer coefficient, kg/m^2 s
k	Thermal conductivity, W/m K
L	Length, m
Le_f	Lewis factor
m	Mass fraction
$\dot{m}$	Mass flow rate, kg/s
MR	Mass flow rate ratio, $\dot{m}_{sw}/\dot{m}_{da}$
NTU	Number of transfer units
Nu	Nusselt number
Pr	Prandtl number
$\dot{Q}$	Heat transfer rate, W
Re	Reynolds number
RR	Recovery ratio
Sc	Schmidt number
Sh	Sherwood number
T	Temperature, K or °C

Greek Symbols

Δ	Change
ε	Heat exchanger effectiveness
ρ	Density, kg/m^3
ω	Humidity ratio

Subscripts

a	Moist air
b	Bulk
c	Coolant

D	Dehumidifier
da	Dry air
H	Humidifier
i	Inner
in	Inlet state
int	Interface
o	Outer
out	Outlet state
p	Product, or fresh water
sat	Saturated
sw	Saline water
v	Water vapor
w	Wall
wb	Wet bulb

Superscripts

$*$	Normalized quantity
sw	Evaluated at the saline water conditions

1 Introduction

1.1 The humidification-dehumidification cycle

Humidification-dehumidification (HDH) is a promising, small-scale desalination system designed to be used in off-grid settings at the community level. It functions much like the natural rain cycle. As shown in Figure 1, warm seawater is sprayed over a packed bed, where it encounters dry air in counterflow. The dry air is humidified by vaporizing pure water from the falling film of seawater. This warm, moist air exits the humidifier and enters the dehumidifier, where the pure water vapor is condensed on cold coils cooled by incoming feed; the feed seawater is preheated in the process. Heat input at the top of the cycle is provided by a water heater. This particular embodiment of HDH is known as a closed air open water (CAOW) cycle. Several other embodiments exist and have been studied in detail [1], but will not be discussed further here.

HDH has several advantages. Its components are simple, effective, and robust, capable of desalting high-salinity waters and requiring only minimal maintenance. By evaporating water at the partial pressure of vapor in air, the top temperature of HDH is naturally reduced (when compared to pure water), and as a result can be run using lower-temperature heat sources. Despite these advantages, and much work on improving the performance of the system through thermodynamic cycle analyses [2–4], HDH remains economically infeasible in many settings as a result of its relatively low energetic performance

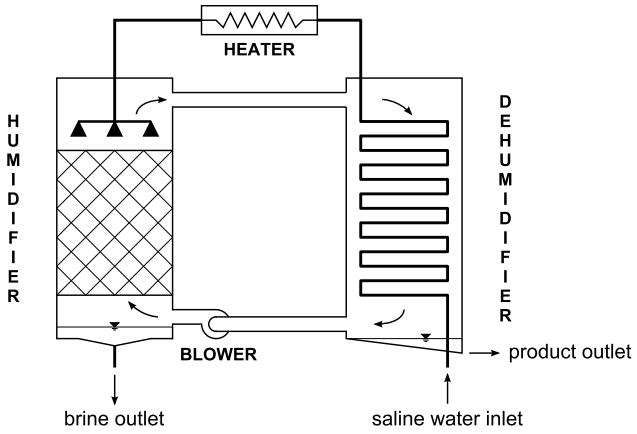

Figure 1: A schematic diagram of closed air open water humidification-dehumidification desalination system.

(as quantified by performance parameters discussed below).

1.2 Overview of extractions and injections in HDH

Employing a technique analogous to balancing a heat exchanger, several authors [5–10] have shown the potential to reduce the irreversibilities—and thereby increase energetic performance—of HDH by altering an effective capacity rate ratio along the length of the humidifier and dehumidifier. Owing to the effect of phase change (*i.e.*, humidification and dehumidification) on the moist air stream's effective capacity rate, Narayan *et al.* [8] and McGovern *et al.* [9] have proposed using mass extractions and injections to increase the efficacy of balancing. In an extraction from the dehumidifier, this involves redirecting a portion of the water stream at some midpoint in the unit and injecting that extracted stream into the humidifier. The injection point is determined by the temperature at which the extraction occurs. That is, in order to minimize any resulting irreversibility associated with the mixing of two streams of differing temperatures, the temperature of the extraction in the dehumidifier should be identical to that of the injection site in the humidifier. Extractions and injections of the air stream and in the reverse direction (humidifier to dehumidifier) may also be employed (see, *e.g.*, [11]); the goal is only to alter the effective capacity rate of either the water or air stream.

Extraction and injection can minimize entropy generation by reducing flow imbalances, or remnant irreversibilities [12]. These imbalances—equivalent to departures from a uniform distribution of driv-

ing temperature or concentration difference [13]—increase entropy production beyond the minimum value for a finite-sized system. This is analogous to a balanced counterflow heat exchanger (or regenerator): here, a balanced heat *and* mass exchanger is desirable to minimize heat input to the HDH cycle. However, unlike the balanced heat exchanger, phase change alters the enthalpy flow rate (and the effective heat capacity rate) of the moist air stream. This means that, unlike a heat exchanger, flow imbalances in a heat and mass exchanger cannot be controlled only by manipulation of the stream-to-stream mass flow rate ratio. Instead, extractions or injections are used to counterbalance the changes in the moist air enthalpy flow rate that result from phase change.

Previous studies of extraction and injection in HDH have shown considerable promise, but all have been purely thermodynamic in nature. The components are modeled using either effectiveness-based, control volume methods or are models based on following a saturation curve process path in both humidification and dehumidification. Thus, the models have not considered the transport process and area requirements of the components. In order to quantify the effects of extraction and injection on a fixed system, the transport processes must be modeled directly. Further, when compared to an effectiveness-based model, a model that includes transport ensures that Second Law violations cannot occur within the component model.

1.3 Performance metrics in desalination

Energetic performance in thermal desalination systems is often quantified by a parameter known as the gained output ratio, or GOR:

$$\mathrm{GOR} = \frac{\dot{m}_p h_{fg}}{Q_{\mathrm{in}}} \tag{1}$$

where $\dot{m}_p$ is the mass flow rate of product (fresh) water, h_{fg} is the specific enthalpy of vaporization, and Q_{in} is the net heat input to the system. The parameter effectively measures how many times the latent heat of condensation is recycled to evaporate additional water.

The objective of the present work is to maximize GOR through mass extractions and injections which reduce irreversibilities. The strong relationship between increased GOR and reduced entropy production can be shown analytically from control volume–based thermodynamic analyses (see, *e.g.*, [14, 15]), and has been studied in great detail for a variety of desalination systems by Mistry *et al.* [16]. Conceptually, this connection is no different from similar ideas found in power systems—maximum work output is obtained when irreversibilities are minimized.

Another important performance parameter is the recovery ratio, defined as the mass of fresh water produced per unit feed, or saline water:

$$\mathrm{RR} = \frac{\dot{m}_p}{\dot{m}_{sw,\mathrm{in}}} \tag{2}$$

In this work, it is shown that for a fixed-size system with fixed boundary conditions, mass extractions and injections can increase GOR at the cost of a slightly decreased recovery ratio. The impact of system size on GOR and water production are also discussed.

2 Model and Numerical Implementation

In this section, models for transport within the humidifier and dehumidifier are introduced, followed by a discussion on their numerical implementation and code validation.

2.1 Humidifier

A packed bed humidifier functions much like a cooling tower, but with a different objective. The goal in the humidifier is to increase the vapor content of the air rather than cool the water. Warm water is sprayed over a packed bed and falls through the packing. Dry air flows upward through the packing; evaporation from the liquid surface causes the air to be heated and humidified while the water cools.

Equations describing the humidifier are given by the well-established Poppe model [17] for cooling towers, as given by Kloppers [18], with mass transfer coefficients provided by Onda [19]. An incremental change in humidity along the streamwise coordinate x is given by

$$\frac{d\omega}{dx} = \frac{KaA_c}{\dot{m}_{da}}(\omega_{\mathrm{sat}}^{sw} - \omega) \tag{3}$$

where K is a mass transfer coefficient, a is the packing specific area (square meters of packing surface per cubic meter of packing volume), A_c is the cross-sectional area of the packing, $\dot{m}_{da}$ is the dry air mass flow rate, and ω is the humidity ratio. Subscript sat indicates that the property should be evaluated at saturation conditions; the superscript sw indicates that the property should be evaluated at the temperature of the saline water. For example, the quantity

ω_{sat}^{sw} is the humidity ratio evaluated at a drybulb temperature equal to the saline water at that location and a relative humidity of one.

The equation describing changes in air enthalpy is

$$\frac{dh_a}{dx} = \frac{KaA_c}{\dot{m}_{da}} \left[\text{Le}_f(h_{a,\text{sat}}^{sw} - h_a) + (1 - \text{Le}_f)h_v^{sw}(\omega_{\text{sat}}^{sw} - \omega)\right] \quad (4)$$

where Le_f is the Lewis factor and h is specific enthalpy per unit mass of dry air. Subscripts a and v indicate moist air and water vapor properties, respectively. As with the convention in equation (3), the term h_v^{sw} is the specific enthalpy of water vapor evaluated at the bulk saline water temperature. (The resistance of the film is negligible compared to the air-side resistance; thus the interface temperature is assumed equal to the bulk water temperature.)

The Lewis factor [20] represents the relative relationship between rates of heat and mass transfer in the system. In the form given by Bošnjaković [21], it is

$$\text{Le}_f = \frac{h_{\text{conv},a}}{c_{p,a}K} = 0.865^{2/3} \frac{\frac{\omega_{\text{sat}}^{sw}+0.622}{\omega+0.622} - 1}{\ln\left(\frac{\omega_{\text{sat}}^{sw}+0.622}{\omega+0.622}\right)} \quad (5)$$

where h_{conv} is a convective heat transfer coefficient, c_p is the specific heat capacity, 0.865 is the Lewis *number*, taken as constant, and 0.622 is the water-to-air ratio of molecular weights. The Lewis number, Le, is the ratio of thermal diffusivity to mass diffusivity.

Finally, changes in bulk saline water temperature are given by

$$\frac{dT_{b,sw}}{dx} = \frac{1}{c_{p,sw}\text{MR}} \left(\frac{dh_a}{dx} - h_{sw}\frac{d\omega}{dx}\right) \quad (6)$$

where MR is the mass flow rate ratio. The mass flow rate ratio the quotient of seawater and dry air mass flow rates:

$$\text{MR} = \frac{\dot{m}_{sw}}{\dot{m}_{da}} \quad (7)$$

2.2 Dehumidifier

In order to obtain basic conclusions about the effects of extraction and injection on 1-D temperature and humidity profiles in the dehumidifier, a very simple tube-in-tube device is considered. In this configuration, coolant flows through an inner tube, while the moist air flows counterflow in the surrounding annulus. This flow geometry is shown in Figure 2.

The warm, moist air that enters the dehumidifier encounters a cold wall. If the temperature of the wall is lower than the local dewpoint, condensation occurs. Otherwise, the air is cooled sensibly. Because the condensate film is impenetrable to the noncondensable gas (*i.e.*, dry air), condensation leads to the accumulation of noncondensable gas near the liquid surface in the usual way. The flow of water vapor toward the interface convects air with it, raising the concentration of air near the interface until counter-diffusion of air offsets the convective flow, creating a stationary air layer at the liquid surface. Along with the sensible heat associated with the cooling of the air, the latent heat released by condensation is conducted through the film, then the wall, and finally into the coolant-side boundary layer. These transport processes are modeled using heat and mass transfer resistance networks, shown schematically in Figure 3 and defined in Table 1. A current source is used in the heat transfer resistance network to represent the enthalpy change associated with the condensing vapor that is absorbed as sensible heat by the coolant.

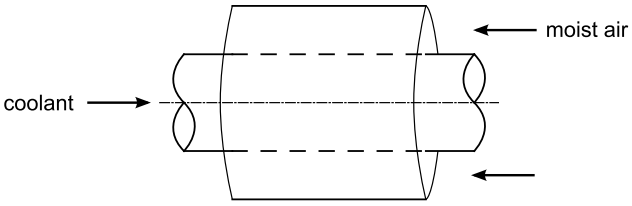

Figure 2: A schematic diagram of a tube-in-tube, counterflow condenser flow geometry.

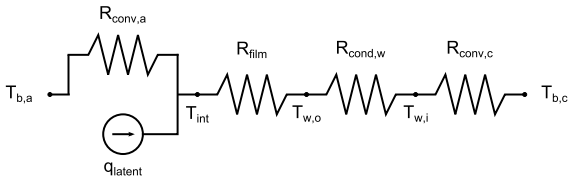

(a) Heat transfer

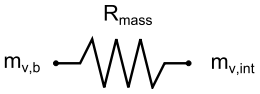

(b) Mass Transfer

Figure 3: Heat and mass transfer resistance networks for the tube-in-tube dehumidifier.

Convective heat transfer coefficients are calculated from the Dittus-Boelter equation for fully-turbulent convective heat transfer. The Nusselt number is

$$\text{Nu}_D = 0.023\text{Re}_D^{0.8}\text{Pr}^n = \frac{h_{\text{conv}}D}{k} \quad (8)$$

Table 1: Dehumidifier resistances.

Resistance	Definition
$R_{\text{conv},a}$	$\dfrac{1}{h_{\text{conv},c}\pi D_{\text{film}}}$
R_{film}	$\dfrac{\ln(D_{\text{film}}/D_o)}{2\pi k_{\text{film}}}$
$R_{\text{cond},w}$	$\dfrac{\ln(D_o/D_i)}{2\pi k_w}$
$R_{\text{conv},sw}$	$\dfrac{1}{h_{\text{conv},c}\pi D_{\text{film}}}$
R_{mass}	$\dfrac{1}{h_{\text{mass}}\pi D_{\text{film}}}$

where $n = 0.4$ for the saline water, or coolant side, $n = 0.3$ for the air side, Re_D is the Reynolds number, Pr is the Prandtl number, D is the appropriate hydraulic diameter, and k is the thermal conductivity. This correlation is applicable only for $\text{Re} \gtrsim 10000$, and all simulations presented here fall within that range. Under the condition considered here, the mass transfer is low rate (*i.e.*, primarily diffusive) and so the air-side mass transfer coefficient is obtained using the analogy between heat and mass transfer. A detailed justification for employing the analogy and the bounds for its use in HDH dehumidifiers are given by Thiel and Lienhard [13]. Using the analogy, the Sherwood number is

$$\text{Sh}_D = 0.023\text{Re}_D^{0.8}\text{Sc}^n = \frac{h_{\text{mass}}D}{\rho\mathscr{D}_{va}} \tag{9}$$

where h_{mass} is the mass transfer coefficient, ρ is the mixture density and $\mathscr{D}_{va}$ is the diffusivity of water vapor in air.

The conservation equations are as follows. Species conservation requires that the vapor condensing at the interface be balanced by changes in humidity of the air stream:

$$\frac{d\omega}{dx} = -\frac{\pi D_o h_{\text{mass}}}{\dot{m}_{da}}(m_{b,v} - m_{\text{int},v}) \tag{10}$$

where $m_{b,v}$ and $m_{\text{int},v}$ are the vapor mass fractions in the bulk and at the interface, respectively. The film/boundary layer interface is saturated, so the quantity $m_{\text{int},v}$ is dictated by temperature alone. A streamwise bulk energy balance on the moist air stream gives

$$\frac{dh_a}{dx} = -\frac{\pi D_o}{\dot{m}_{da}}\Big[h_{\text{conv},a}(T_{b,a} - T_{\text{int}}) - h_{fg}h_{\text{mass}}(m_{b,v} - m_{\text{int},v})\Big] \tag{11}$$

where D_o is the outer diameter of the inner tube,[1] $T_{b,a}$ is the bulk air temperature, and T_{int} is the interface temperature. Energy conservation on the coolant side requires

$$\frac{dh_{sw}}{dx} = \frac{h_{\text{conv},sw}\pi D_i(T_{w,i} - T_{b,sw})}{\dot{m}_{sw}} \tag{12}$$

where $\dot{m}_{sw}$ is the mass flow rate of the saline coolant stream, $T_{w,i}$ is the wall temperature on the inside surface of the inner tube, $T_{b,sw}$ is the coolant bulk temperature, and D_i is the inner diameter of the inner tube. Neglecting the small film resistance, the latent and sensible heat associated with cooling and dehumidification of the moist air stream must both be transferred through the tube wall and be absorbed sensibly by the coolant. Thus,

$$q' = D_o\Big[h_{\text{conv},a}(T_{b,a} - T_{\text{int}}) - h_{fg}h_{\text{mass}}(m_{b,v} - m_{\text{int},v})\Big] \tag{13}$$

$$= \frac{(T_{w,o} - T_{w,i})\,2k_w}{\ln D_o/D_i} \tag{14}$$

$$= h_{\text{conv},sw}D_i(T_{w,i} - T_{b,sw}) \tag{15}$$

where $T_{w,o} = T_{\text{int}}$ because the film resistance has been neglected.

2.3 Heater

The heat input to the cycle is given by

$$\dot{Q}_{\text{in}} = \dot{m}_{sw}\left(h_{sw,H,\text{in}} - h_{sw,D,\text{out}}\right) \tag{16}$$

where the subscripts H and D represent the humidifier and dehumidifier, respectively. The physical size of the heater is not considered here, as mass extractions and injections do not rely upon the physical design of the heater directly. Rather, the cycle heat requirement decreases when mass extractions and injections are implemented. Also, the heater configuration depends on the heat source (*e.g.*, solar, steam, etc.), which is unrelated to the injection and extraction process.

2.4 Thermophysical Properties

Values of moist air enthalpy are per unit dry air, calculated according to the formulation given by Hyland and Wexler [22]. Thermodynamic properties of water and steam are from Harr *et al.* [23]; values of thermal conductivity are given by [24]. The diffusivity of water vapor in air is computed using the correlation of

[1] Here we assume the liquid film to be thin relative to the diameter of the tube.

Marrero and Mason [25]. Although the presence of dissolved solids (salts) alters the vapor pressure, density, and specific heat of water, the use of seawater properties has not been employed here; the relatively minor impact of this approximation for the purposes of understanding the optimization of thermal performance in HDH systems has been explored in detail by McGovern *et al.* [9].

2.5 Solution Procedure

Equations (3)–(6), for the humidifier, and equations (10)–(12), for the dehumidifier, can be integrated for fixed values of dry air and coolant mass flow rates, humidifier and dehumidifier geometries, inlet saline water temperature, humidifier inlet humidity ratio, and humidifier water inlet. Extractions/injections were implemented by altering the seawater mass flow rate up and down stream of the extraction/injection point in accordance with the flowrate of the extraction. This boundary value problem was solved using an iterative technique. Finite differences were implemented in Engineering Equation Solver (EES) [26], a simultaneous solver capable of handling numerous simultaneous, nonlinear algebraic and/or differential equations. Convergence in EES is based on two criteria: (1) the relative residuals are less than 10^{-6}, and (2) the change in variables is less than 10^{-9}. These are the default values in EES. A relative residual is the difference between the two sides of an equation divided by the magnitude of the left hand side. In the case of divergent solutions, EES halts its solving routine after a specified time has elapsed or a predefined number of iterations has been reached.

2.6 Validation

In order to validate the numerical implementation, several comparisons with experimental data and known limiting cases were performed. The implementation of the humidifier model is validated by a comparison to experimental data for cooling towers and an industrial packing manufacturer. Owing to a lack of experimental data for tube-in-tube condensers, the dehumidifier implementation is validated using several limiting cases.

As no experimental data were found for packed bed humidifiers in the operating range of typical HDH systems, the humidifier model implementation was benchmarked against data from cooling towers. Predicted outlet drybulb, wetbulb, and water temperatures were compared to experimental cooling tower data presented by Sharqawy and Husain [27, 28]. As shown in Table 2, the results from the present work agree within 0.5 °C of the experimental values.

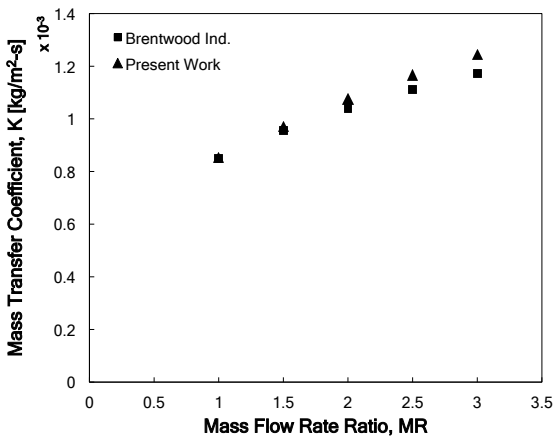

Figure 4: A comparison of experimental values of average mass transfer coefficients for an industrial packing with predictions from Onda's correlation [19].

The use of Onda's mass transfer coefficient correlation was validated using a comparison between data from Brentwood Industries, a manufacturer of packings used in HDH systems (*e.g.*, [11]). Average mass transfer coefficents from a Brentwood CF-1900SB/MA packing and the present work are plotted against mass flow rate ratio for a fixed set of inlet conditions in Figure 4; values from the present work agree within approximately 6%.

To the authors knowledge, no suitable data are available for the validation of tube-in-tube dehumidifiers. This is fully a result of the dehumidifier models used here: in practice, a shell-in-tube configuration provides a far more compact geometry and is used almost exclusively in practice. As a result, the model is instead compared to well-known, limiting cases in heat transfer theory.

In the limiting case of zero inlet humidity, no condensation occurs, and the model reduces to a simple, two-stream, counterflow heat exchanger. For water and air inlet temperatures of 30 °C and 70 °C, respectively, a capacity rate ratio ($C^* = (\dot{m}c_p)_{\min}/(\dot{m}c_p)_{\max}$) of unity, and a number of transfer units (NTU) of 2.96, the dehumidifier model predicts an effectiveness of $\varepsilon = 0.755$. For this NTU, heat exchanger theory predicts an effectiveness of 0.747—a difference of about 1%. As shown in Figure 5, several data points plotted along with the effectiveness versus NTU curve for a balanced heat exchanger confirm this good agreement.

In the case where one mass flow rate greatly ex-

Table 2: A comparison of results from the humidifier model and experimental data from [27, 28].

	Experimental data [°C]			Present Work [°C]			Absolute Error [°C]		
MR	$T_{a,\text{out}}$	$T_{wb,\text{out}}$	$T_{\text{water, out}}$	$T_{a,\text{out}}$	$T_{wb,\text{out}}$	$T_{\text{water, out}}$	$T_{a,\text{out}}$	$T_{wb,\text{out}}$	$T_{\text{water, out}}$
1.0	25.8	23.7	25.5	25.8	24.0	25.6	0.0	0.3	0.1
1.5	26.9	24.0	27.1	26.5	23.8	27.5	0.4	0.2	0.4
2.0	27.6	24.5	28.2	27.1	24.6	28.4	0.5	0.1	0.2

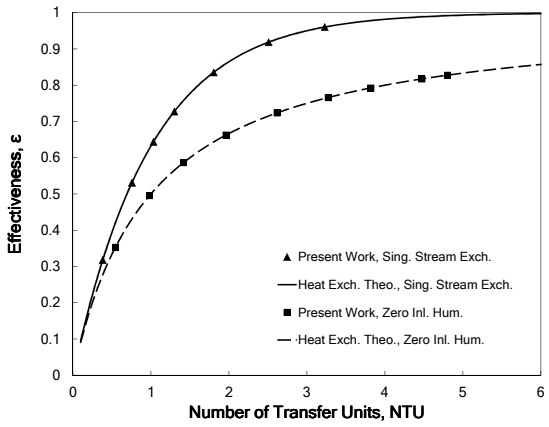

Figure 5: A comparison of effectiveness vs. NTU for the cases of zero inlet humidity and a high mass flow rate ratio with results from heat exchanger theory.

ceeds the other, the high mass flow rate stream becomes roughly isothermal. Choosing a high airside mass flow rate thus avoids the complex effects of condensation on the airside temperature profile, and the problem reduces to a single stream exchanger. For water and air inlet temperatures of 40 °C and 60 °C, respectively, MR = 0.1 and an NTU of 3.00, the model predicts an effectiveness of 0.949. Heat exchanger theory predicts an effectiveness of 0.950—a difference of less than 1%. Similar results are shown in Figure 5, a plot of effectiveness versus NTU; data points from the present work fall nearly exactly along the line prescribed by heat exchanger theory for a single stream exchanger.

3 Results and Discussion

The impact of mass extractions and injections on cycle performance, quantified by GOR, is discussed first, followed by the effect of system size on thermal performance and water production.

Table 3: Cycle model inputs.

Parameter	Value
Humidifier Area [m^2]	455
Dehumidifier Area [m^2]	4.88
Humidifier Water Inlet Temp. [°C]	58.6
Humidifier Air Inlet RH	1
Dehumidifier Water Inlet Temp. [°C]	30
Dry Air Flow Rate [kg/s]	0.03
Mass Flow Rate Ratio	2.44

3.1 Effect of Extraction/Injection on GOR and Water Production

Several parametric studies were performed to identify the impact of a single mass extraction/injection from the dehumidifier to the humidifier on a system of fixed size and fixed inlet conditions. The values for a representative high GOR case are shown in Table 3. These particular temperature and humidity inputs were chosen based on values for an optimized cycle without extractions from Mistry *et al.* [4]. Although the model by Mistry *et al.* was effectiveness based, component sizes were chosen roughly to match the assumed values of effectiveness used in that work.

Inspection of temperature and vapor fraction profiles for this base case, as shown in Figure 6, confirms the assertions made in Section 1.2. The phase change processes occurring at various rates along the length of both humidifier and dehumidifier drive the process paths away from more familiar linear or exponential temperature curves typical of heat exchangers. Compared to a standard, single-phase, two-stream heat exchanger, the challenge of balancing these heat and mass exchangers is thus readily apparent—changes to the distributions of driving temperature and concentration difference must be effected mid-stream, and not simply at the terminals. Furthermore, due to the counterflow arrangement, the parameters that must be altered along the length to balance the HME affect properties both up and downstream of the extraction/injection point.

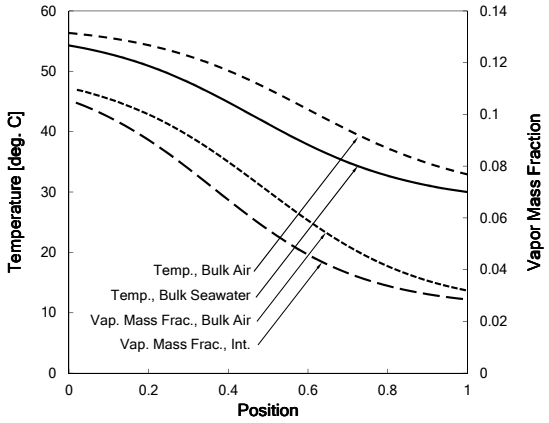

(a) Dehumidifer

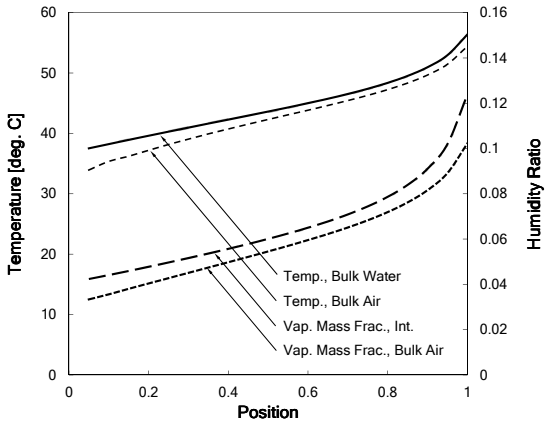

(b) Humidifier

Figure 6: Temperature and vapor concentration profiles in the dehumidifier and humidifier for the baseline case of zero extractions.

Table 4: GOR values for several combinations of extraction flow rate and extraction temperature.

Extraction flow % of circuit flow	Extraction Temperature [°C]	GOR –
0 %	–	5.33
10 %	55.4	5.50
10 %	50.6	5.49
10 %	46.5	5.32
10 %	40.5	5.23
20 %	53.1	5.65
20 %	50.1	5.62
20 %	45.6	5.14
20 %	40.3	4.84

Qualitatively, the profiles reveal no obvious points at which to extract or inject. The extraction flow rate and the temperature at which flow was extracted was thus varied. In order to minimize any entropy production associated with mixing two streams in thermal disequilibrium, the temperature at the injection location on the humidifier was matched to the temperature of the extracted stream. Note, however, that matching these two locations requires some computational effort, as the redirection of a portion of the coolant stream from the dehumidifier to the humidifier affects conditions both upstream and downstream of the extraction/injection point. Representative values of GOR for various combinations of extraction/injection flow rate and temperature in Table 4 show the trend: compared to the baseline value of GOR, extracting at a higher temperature has a greater impact on GOR than at lower temperatures. This result can be attributed to the exponential dependence of saturation humidity on absolute temperature. At higher temperatures, in both the humidifier and dehumidifier, the interfacial humidity changes more rapidly; the significance of changing the effective capacity rate is thus more pronounced at those higher temperatures. The resulting, more balanced system is more reversible, and thus has an increased GOR.

Temperature and vapor concentration profiles for a simulation with an extraction, shown in Figure 7, display an obvious 'kink' in the graph where an extraction or injection has been made. This confirms the goal of extraction and injection—the ability to modify the slopes of the two process paths along the length, change the effective heat capacity rate, and alter the average driving force and distribution of driving forces within the system to increase performance.

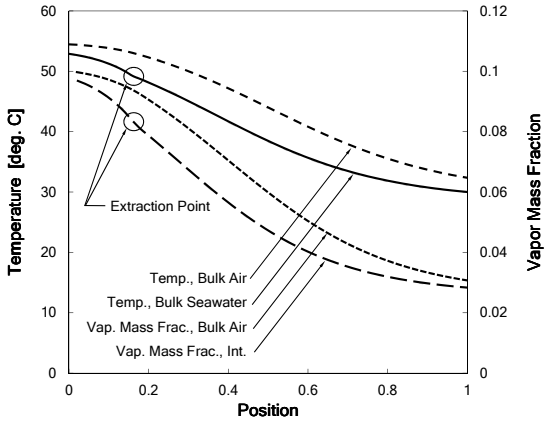

(a) Dehumidifer

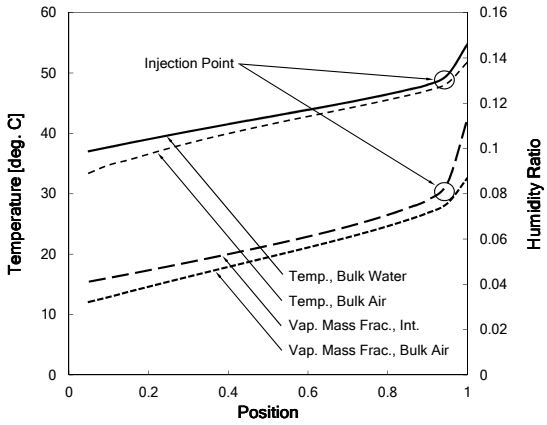

(b) Humidifier

Figure 7: Temperature and vapor concentration profiles in the dehumidifier and humidifier for the optimum case of a 40% water flow extraction/injection.

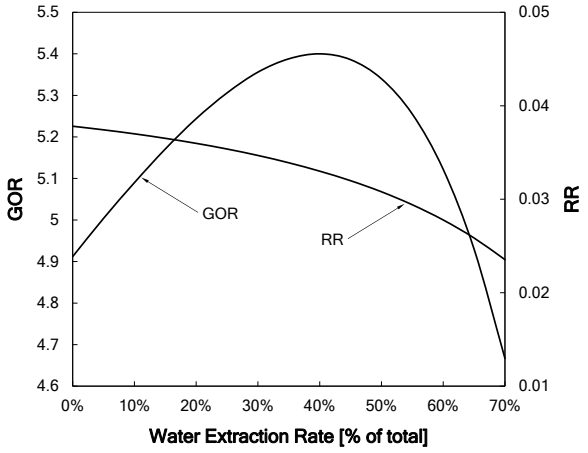

Figure 8: GOR and RR vs. extraction flow rate.

For a given extraction temperature, the effect of extraction/injection flow rate is shown in Figure 8. An optimal extraction mass flow rate that produces the highest GOR—an approximately 10% increase over the baseline case—is found to be about 40% of the inlet water (saline feed) flow rate. This optimum is a result of balancing the dehumidifier—when too much flow is extracted, the dehumidifier is effectively 'unbalanced' and irreversibilities are increased 1rather than reduced. At that point, systemwide irreversibility again increases, heat recovery is no longer optimized, and GOR decreases.

This conclusion is further corroborated by a plot of the parameters that affect GOR, *viz.*, the heat input and the product mass flow rate, versus the extraction/injection flow rate, as shown in Figure 9. As flow is extracted from the dehumidifier, both the heat input and product flow rate drop; however, the heat input initially drops quicker than the product flow rate. This results in an increase in GOR. These trends can be explained by the temperatures curves shown on Figure 9. As the dehumidifier water outlet temperature (a measure of the preheat) decreases, much of the flow is redirected away from the heater, resulting in a net decrease in required heat input. The range of the cycle (*i.e.*, the difference between top and bottom air temperatures) is reduced, and because the humidity of saturated moist air is a function only of the temperature, the product water flow is also reduced.

Table 5: A comparison of two extraction/injection studies with the present work.

Study	Approach	Major Conclusions
McGovern *et al.*, [9]	• Thermodynamic models for each component • Assumes air follows the saturation curve • Compares the effects of extraction/injection on systems of fixed pinch-point temperature differences	• A single extraction from the humidifier to the dehumidifier can increase GOR by up to a factor of four. • GOR increases and RR decreases as the temperature range of the cycle decreases.
Narayan *et al.*, [8]	• Thermodynamic models for each component • Assumes air follows the saturation curve • Compares the effects of extraction(s)/injection(s) on systems of fixed enthalpy pinch	• A single extraction from the humidifier to the dehumidifier reduces entropy production by up to 60%. • Continuous extraction/injection gives a reversible upper limit on GOR for HDH of 109.7.
Miller and Lienhard, [10]	• Thermodynamic models for each component • Compares the effect of one to five extractions/injections on a system of fixed-sub-component effectivnesses	• One extraction from the dehumidifier to the humidifier increases GOR. • Multiple extractions/injections can, but do not always improve performance.
Present Work	• Transport-based models for each component • Compares the effect of a single extraction/injection on a fixed-size, fixed-boundary-condition system	• A single extraction from the dehumidifier to the humidifier results in an increase in GOR of 10%. • Increasing size increases GOR and water production for the present b.c.'s, whereas extraction/injection may increase GOR, but decrease water production

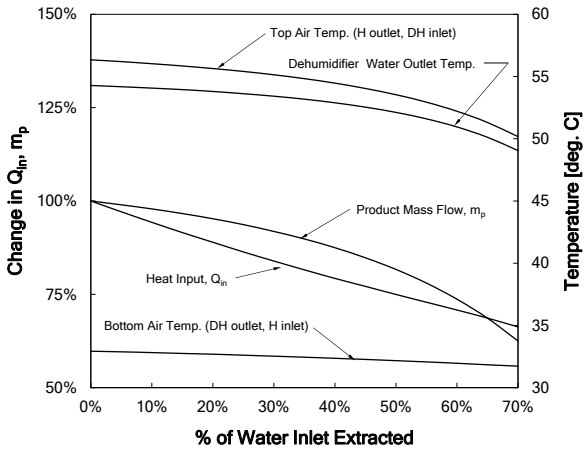

Figure 9: The relative change in heat input and fresh water flowrate, and changes in system temperatures as a function of the percentage of inlet water flow extracted.

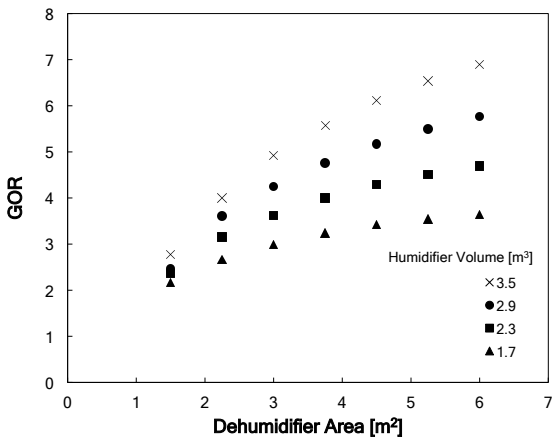

Figure 10: GOR vs. dehumidifier size for given values of humidifier volume.

3.2 Comparison with Previous Studies On Extraction and Injection

As discussed in Section 1.2, several previous studies have examined the effects of extraction and injection in HDH systems. In those past studies, the system size was not fixed (on design approach) so that injection and extraction were performed at fixed component effectiveness; the present study fixes component size while performing injection and extraction (off design approach). The present study differs from those studies in the conclusion that for a fixed size, fixed inlet temperature HDH system, extracting from the dehumidifier and injecting into the humidifier proves more beneficial than doing the reverse. This conclusion is summarized and compared to the previously referenced thermodynamic studies in Table 5. As shown in the table, larger gains in GOR were made in the thermodynamic studies. This comparison is significant because it may imply that better performance gains can be made when considering the addition of extraction and injection in the design step (on design approach) as opposed to simply adding it to an existing system, where top temperature, inlet conditions, size, and other boundary conditions are already fixed (off design approach).

3.3 Effect of System Size on GOR and Water Production

For a given set of boundary conditions, the effect of component size on GOR is shown in Figure 10. As expected, an increase in system size results in smaller driving forces, less irreversibility, and thus a lower heat requirement and higher GOR. Perhaps more interesting, however, is the observation of diminishing returns. As the dehumidifier area is increased, GOR increases first rapidly, but then tapers off. Thus, despite conclusions of previous cycle analyses [16] that have emphasized the importance of reducing irreversibilities in the dehumidifier, in designing a real system, it is important to choose the sizes of both components in a coordinated manner. Increasing the size of a single component serves only to reduce irreversibilities in that component; thereafter, irreversibilities in the other component will dominate and will limit any further increase in performance.

For a given set of boundary conditions, the effect of component size on water production is shown in Figure 11. Compared to the effect on GOR, the effect of size on water production is smaller. Water production increases with larger system sizes, but the magnitude of the increase in water production is only about 70% with a doubling in system size. The relative size of these two trends makes sense in the context of the boundary conditions, however. The top and bottom temperatures of the system are constrained as an input; and for a given dry air flow rate, the maximum water production is constrained by the difference in moist air humidity at these two values of temperature. Thus, only with higher top temperatures and/or higher dry air flow rates will the impact of large changes in area on water production be fully realized.

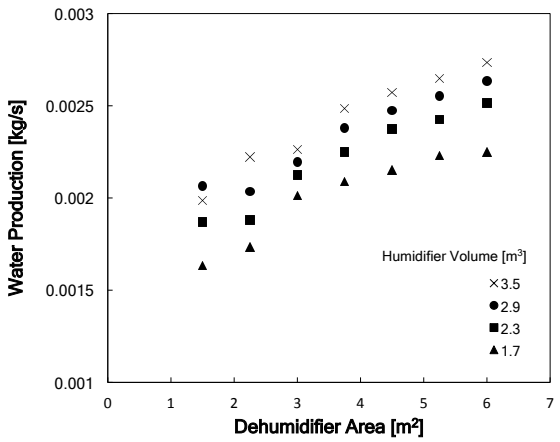

Figure 11: Water production vs. system size.

4 Conclusions

In this work, models describing fixed-size humidifiers and dehumidifiers for use in a humidification-dehumidification desalination system were developed to explore the effects of mass extraction/injection on cycle performance.

The effect of a single extraction from the dehumidifier to the humidifier on a thermodynamically optimized HDH system has been shown to be an increase in GOR of approximately 10%. This direction of extraction/injection is in contrast to previous literature on the topic, in which purely thermodynamic considerations showed the opposite direction to be superior. However, for the fixed boundary conditions and parameters used in this work, (a fixed system size, fixed inlet temperature, and fixed top temperature) extracting from the dehumidifier and injecting into the humidifier is more effective. Varying the temperature at which flow was extracted displayed trends consistent with other literature on the subject—extracting at higher temperatures produced higher values of GOR. The optimal extraction flow rate was found to be about 40% of the total circuit flow.

The effects of system size on GOR and water production rate were also quantified. While an increase in system size reduces cycle heat requirements, a trend of diminishing returns was revealed. Both GOR and water production rate increase as component sizes are increased, but the effect is limited if the size of only one component is increased. For an appropriately-sized humidifier, doubling the area of the dehumidifier can double or triple GOR; water production increases by a smaller margin.

In summary, based on this work and previous works on HDH performance, there are four major factors impacting the GOR of HDH systems with extractions and injections: (1) extraction and injection temperature and mass flow rate; (2) system size; (3) temperature and concentration range of the cycle; and (4) mass flow rate ratio. Because the boundary conditions for the cycle were chosen based on a thermodynamically optimized system without extractions, further optimization work using the present model is required to obtain the maximum performance gain on a fixed-size system with extractions.

Acknowledgements

The authors would like to thank the King Fahd University of Petroleum and Minerals for funding the research reported in this paper through the Center for Clean Water and Clean Energy at MIT and KFUPM under project number R4-CW-08. Gratitude is also extended to Eni and the Martin Family Foundation for fellowship support to the first author.

References

[1] G. P. Narayan, M. H. Sharqawy, E. K. Summers, J. H. Lienhard V, S. M. Zubair, and M. A. Antar, "The potential of solar-driven humidification-dehumidification desalination for small-scale decentralized water production," *Renewable and Sustainable Energy Reviews*, vol. 14, pp. 1187–1201, May 2010.

[2] G. P. Narayan, M. H. Sharqawy, and J. H. Lienhard V, "Thermodynamic analysis of humidification dehumidification desalination cycles," *Desalination and Water Treatment*, vol. 16, no. 1-3, pp. 339–353, 2010.

[3] G. P. Narayan, J. H. Lienhard V, and S. M. Zubair, "Entropy generation minimization of combined heat and mass transfer devices," *International Journal of Thermal Sciences*, vol. 49, no. 10, pp. 2057–2066, 2010.

[4] K. H. Mistry, A. Mitsos, and J. H. Lienhard V, "Optimal operating conditions and configurations for humidification-dehumidification desalination cycles," *International Journal of Thermal Sciences*, vol. 50, no. 5, pp. 779–789, 2011.

[5] M. A. Younis, M. A. Darwish, and F. Juwayhel, "Experimental and theoretical study of a humidification-dehumidification desalting system," *Desalination*, vol. 94, pp. 11–24, 1993.

[6] T. Brendel, *Solare Meerwasserentsalzungsanlagen mit mehrstufiger Verdunstung - Betriebsversuche, dynamische Simulation und Optimierung*. PhD thesis, Ruhr-Universität Bochum, 2003.

[7] H. Müller-Holst, "Solar thermal desalination using the multiple effect humidification (MEH)-method," in *Solar Desalination for the 21st Century* (L. Rizzuti, H. Ettouney, and A. Cipollina, eds.), vol. 18 of *NATO Security through Science Series*, pp. 215–225, Springer Netherlands, 2007.

[8] G. P. Narayan, K. Chehayeb, R. K. McGovern, G. P. Thiel, S. M. Zubair, and J. H. Lienhard V, "Thermodynamic balancing of the humidification dehumidification desalination system by mass extraction and injection," *International Journal of Heat and Mass Transfer*, vol. 57, pp. 756–770, 2013.

[9] R. K. McGovern, G. P. Thiel, G. P. Narayan, S. M. Zubair, and J. H. Lienhard V, "Performance limits of zero and single extraction humidification-dehumidification desalination systems," *Applied Energy*, vol. 102, pp. 1081–1090, 2013.

[10] J. A. Miller and J. H. Lienhard V, "Impact of extraction on a humidification-dehumidification desalination system," *Desalination*. In press.

[11] G. P. Narayan, M. St. John, S. M. Zubair, and J. H. Lienhard V, "Thermal design of the humidification-dehumidification desalination system: an experimental investigation," *International Journal of Heat and Mass Transfer*. In press.

[12] A. Bejan, *Advanced engineering thermodynamics*. John Wiley & Sons, 2006.

[13] G. P. Thiel and J. H. Lienhard V, "Entropy generation in condensation in the presence of high concentrations of noncondensable gases," *International Journal of Heat and Mass Transfer*, vol. 55, pp. 5133–5147, September 2012.

[14] K. H. Mistry, J. H. Lienhard V, and S. M. Zubair, "Effect of entropy generation on the performance of humidification-dehumidification desalination cycles," *International Journal of Thermal Sciences*, vol. 49, no. 9, pp. 1837–1847, 2010.

[15] G. P. Thiel, "Entropy generation minimization of a heat and mass exchanger for use in a humidification-dehumidification desalination system," Master's thesis, Massachusetts Institute of Technology, 2012.

[16] K. H. Mistry, R. K. McGovern, G. P. Thiel, E. K. Summers, S. M. Zubair, and J. H. Lienhard V, "Entropy generation analysis of desalination technologies," *Entropy*, vol. 13, no. 10, pp. 1829–1864, 2011.

[17] M. Poppe, "Wärme- und stoffübertragung bei der verdunstungskühlung im gegen- und kreuzstrom," *VDI-Forschungsheft*, no. 560, 1973.

[18] J. C. Kloppers and D. G. Kröger, "A critical investigation into the heat and mass transfer analysis of counterflow wet-cooling towers," *International Journal of Heat and Mass Transfer*, vol. 48, pp. 765–777, 2005.

[19] K. Onda, H. Takeuchi, and Y. Okumoto, "Mass transfer coefficients between gas and liquid phases in packed columns," *Journal of Chemical Engineering of Japan*, vol. 1, no. 1, pp. 56–62, 1968.

[20] J. C. Kloppers and D. G. Kröger, "The Lewis factor and its influence on the performance prediction of wet-cooling towers," *International Journal of Thermal Sciences*, vol. 44, pp. 879–884, 2005.

[21] F. Bošnakjović, *Technische Thermodynamik*. Verlag, 1965.

[22] A. Wexler, R. Hyland, and R. Stewart, *Thermodynamic Properties of Dry Air, Moist Air and Water and SI Psychrometric Charts*. American Society of Heating, Refrigeration and Air-Conditioning Engineers, Inc., 1983.

[23] L. Harr, J. Gallagher, and G. S. Kell, *NBS/NRC Steam Tables: Thermodynamic and Transport Properties and Computer Programs for Vapor and Liquid States of Water in SI Units*. Hemisphere Press, 1984.

[24] Electrical Research Association, *1967 Steam Tables, Thermodynamic Properties of Water and Steam; Viscosity of Water and Steam, Thermal Conductivity of Water and Steam*. Edward Arnold Publishers, 1967.

[25] T. R. Marrero and E. A. Mason, "Gaseous diffusion coefficients," *Journal of Physical and Chemical Reference Data*, vol. 1, no. 1, pp. 3–118, 1972.

[26] S. A. Klein, *Engineering Equation Solver*. F-Chart Software, LLC.

[27] I. Husain, "Performance evaluation of seawater counter flow cooling towers," Master's thesis, King Fahd University of Petroleum and Minerals, 2011.

[28] M. H. Sharqawy, I. S. Husain, S. M. Zubair, and J. H. Lienhard V, "Thermal performance evaluation of seawater cooling towers," in *Proc. ASME 2011 Intl. Mech. Engr. Cong. & Exp.*, (Denver), November 2011.